International Journal of Cardiology 287 (2019) 32–38

Contents lists available at ScienceDirect

International Journal of Cardiology

journal homepage: www.elsevier.com/locate/ijcard

Tissue characteristics of culprit lesion and myocardial tissue-level perfusion in non-ST-segment elevation acute coronary syndromes: The EARLY-MYO-ACS study

Gan Yang [a,1], Wei Wang [a,1], Xinchen Sheng [a,1], Fan Yang [a], Linchong Kong [a], Jie He [a], Song Ding [a], Peiren Shan [b], Yunpeng Shang [c], Jianchen Xiu [d], Yining Yang [e], Gary S. Mintz [f], Jun Pu [a,*]

[a] Department of Cardiology, Renji Hospital, School of Medicine, Shanghai Jiaotong University, Shanghai 200127, China
[b] The First Affiliated Hospital of Wenzhou Medical College, Wenzhou 325035, China
[c] The First Affiliated Hospital, Zhejiang University School of Medicine, Hangzhou 310009, China
[d] Nanfang Hospital Southern Medical University, Guangzhou 510515, China
[e] The First Affiliated Hospital, Xinjiang Medical University, Wulumuqi 830054, China
[f] Clinical Trials Center, Cardiovascular Research Foundation, New York, NY, USA

ARTICLE INFO

Article history:
Received 13 May 2018
Received in revised form 1 January 2019
Accepted 7 February 2019
Available online 8 February 2019

Keywords:
Plaque characterization
Intravascular ultrasound
Myocardial tissue-level perfusion
Acute coronary syndrome

ABSTRACT

Objective: The impact of tissue characteristics of culprit lesion on myocardial tissue-level perfusion in non-ST-segment elevation acute coronary syndrome (NSTE-ACS) remains unclear. EARLY-MYO-ACS study was a prospective observational study to investigate the relationship between pre-percutaneous coronary intervention (PCI) culprit plaque characteristics and post-PCI myocardial tissue-level perfusion with iMap intravascular ultrasound (IVUS) in NSTE-ACS patients.

Methods: A total of 408 patients with coronary artery disease (246 NSTE-ACS and 162 stable angina pectoris) undergoing coronary angiography, grayscale-IVUS and iMap-IVUS were enrolled. Tissue characteristics of culprit lesion were analyzed by the iMap-IVUS system as fibrotic, lipidic, necrotic, or calcified tissue. Epicardial coronary perfusion was assessed by TIMI flow grade (TFG), and myocardial tissue-level perfusion was assessed by both TIMI myocardial perfusion grade (TMPG) and TIMI myocardial perfusion frame count (TMPFC).

Results: The percentages of necrotic volume within the culprit lesion were significantly greater in NSTE-ACS than that in stable angina pectoris (20.8 ± 7.9% vs. 15.9 ± 7.2%, $P < 0.001$). Patients with impaired epicardial coronary perfusion (TFG 0–2) had higher necrotic percentage within the culprit lesion than those with normal TFG (27.9 ± 7.3% vs. 19.6 ± 7.4%, $P < 0.001$). Moreover, patients with impaired myocardial tissue-level perfusion (TMPG 0–2) had greater necrotic percentages within the culprit lesion than those with normal TMPG (25.0 ± 8.1% vs. 18.4 ± 6.7%, $P < 0.001$). Multivariate analysis revealed that iMap-derived necrotic volume percentage was independently associated with reduced post-PCI TMPG (OR 2.39 [95% CI 1.60 to 3.57], $P = 0.009$) and impaired post-PCI TMPFC (OR 2.89 [95% CI 1.62 to 5.16], $P = 0.008$). The ROC curve showed that the optimal threshold of necrotic volume percentage was 20.09% and 21.03% to predict impaired TMPG and TMPFC, respectively.

Conclusion: Increased necrotic fraction of the culprit lesion is independently associated with impaired myocardial tissue-level perfusion in NSTE-ACS patients. Thus, plaque composition assessed by pre-PCI iMap-IVUS could predict post-PCI impaired myocardial tissue-level perfusion in NSTE-ACS patients (Trial Registration: ChiCTR-OCH-13003046).

1. Introduction

Percutaneous coronary intervention (PCI) is the most effective strategy to treat patients with non-ST-segment elevation acute coronary syndrome (NSTE-ACS). However, we and other investigators have found that, despite successful recanalization with an apparent normal epicardial coronary flow, a substantial number of patients still fail to achieve complete myocardial tissue-level reperfusion, which contributes to the increased cardiac mortality and morbidity [1–5]. Therefore, identification of the predictors for impaired myocardial tissue-level perfusion is of great importance.

Previous studies have focused on the association between plaque composition and epicardial coronary flow in NSTE-ACS patients, and

* Corresponding author at: Department of Cardiology, Shanghai Renji Hospital, School of Medicine, Shanghai Jiaotong University, Shanghai 200127, China.
E-mail address: pujun310@hotmail.com (J. Pu).
[1] The first three authors contributed equally to this work.

https://doi.org/10.1016/j.ijcard.2019.02.010
0167-5273/

showed that the tissue characteristics of culprit lesion was associated with the epicardial coronary perfusion post-PCI [6]. We and other investigators have shown that a large plaque burden, positive remodeling, lipid pool-like images and echo-attenuated plaques on gray-scale intravenous ultrasound (IVUS) were indicators of impaired epicardial coronary perfusion [7–10]. However, gray-scale IVUS is limited in its assessment of tissue characterization, especially for necrotic core-rich (NC) plaques [7]; and the impact of culprit lesion tissue characteristics on myocardial tissue-level perfusion in NSTE-ACS remains unclear.

iMap-IVUS imaging system is the most recent radiofrequency IVUS imaging system which acquires radiofrequency data and color-codes coronary plaque as either green (fibrous), yellow (lipidic), red (necrotic), or blue (calcified). Sathyanarayana et al. found that iMap-derived coronary plaque composition in vivo was closely correlated with the results of histopathological examination of tissue samples obtained by directional coronary atherectomy [11]. The EARLY-MYO-ACS study was a prospective observational registry to investigate the relationship between pre-PCI culprit plaque characteristics and post-PCI myocardial tissue-level perfusion in NSTE-ACS patients using the iMap-IVUS imaging system.

2. Materials and methods

2.1. Study design and patients

EARLY-MYO-ACS study was a prospective observational registry (ChiCTR-OCH-13003046) designed to investigate the impact of pre-PCI early assessment of plaque tissue characteristics on post-PCI myocardial tissue-level perfusions in NSTE-ACS patients using the iMap-IVUS imaging system. From May 2016 to April 2017, 246 consecutive patients with NSTE-ACS were included in the study. The inclusion criteria were consecutive patients' age > 18 years old with NSTE-ACS who were referred for PCI of a native, de novo coronary lesion. Each lesion selected for imaging was a culprit or target lesion undergoing planned PCI. Key exclusion criteria were ST-segment elevation myocardial infarction (STEMI), previous revascularization (PCI or bypass surgery), any contraindication for PCI, and life expectancy <2 years. Data of angiograms and grayscale IVUS and iMap-IVUS were prospectively entered into the study database. During the same enrollment period, the data of SAP patients who were referred for PCI of a native, de novo coronary lesion and who had a documented culprit lesion identified by invasive/noninvasive functional or ischemic testing were also consecutively entered into the study database to further plaque characteristics comparison between NSTE-ACS and SAP patients. This study was performed in accordance with the Declaration of Helsinki. The study protocol was approved by the Institutional Review Board. Informed consent was obtained from all patients before the procedure.

2.2. Coronary angiography and IVUS procedure

The detailed procedure was described in our supplementary material.

2.3. Angiographic analysis

Angiographic data were analyzed off-line in an independent core angiographic laboratory with a computer-based cardiovascular angiographic analysis system by two independent, experienced angiographers who were blinded to all data apart from the coronary angiograms [2]. Epicardial coronary flow in the culprit artery was graded according to the Thrombolysis in Myocardial Infarction (TIMI) flow grade [12]. Myocardial tissue-level perfusion was assessed by both the TIMI myocardial perfusion (TMPG) [13] and the TIMI myocardial perfusion frame count (TMPFC) [1,2]. TMPFC is a newly developed method to standardize and quantify myocardial perfusion by timing the filling and washout of contrast in the myocardium using cine-angiographic frame-counting as previously described [1,2]. Briefly, the first frame of TMPFC was defined as the frame that clearly demonstrated the first appearance of myocardial blush beyond the infarct-related artery (IRA) (F1). The last frame of TMPFC was then defined as the frame where contrast or myocardial blush disappeared (F2). TMPFC was calculated as F2 minus F1 frame counts at a filming rate of 15 frames/s, or (F2 minus F1) * 2 frame counts at the corrected filming rate of 30 frames/s. The left anterior descending artery and left circumflex artery were usually best assessed in the left anterior oblique views with caudal angulations. The right coronary artery was usually best assessed in the left anterior oblique projection with steep cranial angulation.

2.4. Analysis of intravascular ultrasound images

Grayscale IVUS analysis was performed according to criteria from American College of Cardiology (ACC) consensus statement on IVUS [14]. The borders of the vessel and lumen were identified by automatic edge detection and corrected manually when necessary. External elastic membrane (EEM) and lumen cross-sectional areas (CSA) were measured. Plaque plus media (P&M) CSA was calculated as EEM minus lumen CSA; and plaque burden was calculated as P&M divided by EEM CSA. Remodeling index was the ratio of lesion site EEM CSA divided by the average of the proximal and distal reference EEM CSA. The plaque classification was based on three consecutive frames with a plaque burden >40%. Qualitative assessments of grayscale-IVUS plaque morphology were based on the echogenic characteristics of the plaque on the cross-sectional view, and the adventitia was used as a reference for echo-reflectivity [15]. Echo-attenuated plaque was defined as >30° ultrasonic attenuation in three consecutive frames despite the absence of bright calcium [15]. Echolucent plaque was defined as a large echolucent zone (thickness >0.3 mm) surrounded by tissue of greater echogenicity and was closer to the luminal surface than to the adventitia (shallow location). Calcified plaque was defined as hyperechoic plaque with acoustic shadowing. Plaque rupture was defined as an intraplaque cavity in the vessel wall, with disruption of the intima, and flow observed within the plaque cavity [14].

We assessed plaque composition for both the minimum lumen area (MLA) site and the entire culprit lesion. Qualitative and quantitative analysis of each plaque was done with iMap software (Boston Scientific) and QIvus software (Medis Medical Imaging Systems). In brief, the iMap system performed spectral analysis of IVUS radiofrequency data and classified each plaque into 4 color-coded components (green = fibrous, yellow = lipidic, pink = necrotic, and blue = calcified). The lumen and the media-adventitia interface were outlined by automatic edge detection and corrected manually for the entire culprit lesion. Volumes were calculated using Simpson's rule. The volume of each component was then calculated from cross-sections of 0.5 mm each covering the entire lesion. The percentage of each tissue component was calculated as the volume of each divided by the total plaque volume. Plaque with acoustic shadowing, severe calcification, or wire artifact was unsuitable for analysis and thus automatically removed. The data were stored on a hard disk for offline analysis that was performed independently by experienced analysts who were blinded to all data apart from IVUS.

2.5. Statistical analysis

2.5.1. Sample size calculation

The primary hypothesis of the present study was that NSTE-ACS patients with impaired myocardial tissue-level perfusion (i.e., TMPG <3) would had greater necrotic percentages within the culprit lesion than those with normal myocardial perfusion. According to the data provided by the published literatures on the association of culprit lesion characteristics and epicardial coronary perfusion [6,16,17] and assuming that the necrotic percentages in impaired TMPG group was 22% and 14% in the normal TMPG group, the sample sizes required was a total of 230 NSTE-ACS patients to allow detection of an 8% difference in the necrotic percentages within the culprit lesion in impaired vs. normal TMPG patients with 85% power and a 2-sided α value of 0.05.

2.5.2. Final analysis

Statistical analyses were performed using SAS9.13. In our presentation of the data, continuous baseline and outcome variables were given as the mean ± SD, while discrete variables were given as absolute values, percentages, or both. Continuous variables were compared using the Student's *t*-test if normally distributed and the Wilcoxon rank-sum if not. To examine the normal distribution, the Shapiro-Wilk test was used. Categorical variables were compared using chi-square with normal approximation or Fisher's exact test when appropriate. Logistic regression analysis was performed to evaluate the significance of risk predictors of impaired angiographic microvascular flow. Two criteria were considered necessary for a variable to be entered in the model: i) a univariate *P* value for myocardial tissue-level perfusion of 0.10 or less; and ii) a plausible association with the risk of impaired myocardial perfusion or the incidence of MACE according to data provided by the literature. Odds ratios and 95% confidence intervals were calculated. A two-tailed *P*-value of <0.05 was considered to be statistically significant for all analyses. Correlation between NC% and TMPFC was evaluated by using linear regression models. Receiver-operator characteristics (ROC) curve were generated from multiple sensitivity/specificity pairs. The optimal cutoff point was defined the point on the ROC curve closest to (0, 1).

3. Results

3.1. Baseline characteristics of the enrolled patients

We prospectively enrolled 246 NSTE-ACS patients who had pre-PCI angiogram, grayscale and iMap-IVUS, and underwent PCI in the present study. Meanwhile, 162 patients with SAP who had pre-PCI angiogram and grayscale and iMap-IVUS were enrolled as control. The flow chart of patients' enrollment process was shown in the Fig. 1. There were no differences in the prevalence of classical coronary risk factors between NSTE-ACS and SAP groups except the current smoking rate ($P < 0.001$) (Table 1). Compared with the SAP group, patients with NSTE-ACS had lower left ventricle ejection fraction ($P = 0.002$). There were no significant differences between the 2 groups with regard to the distribution of culprit arteries, rates of stent implantation, or number of implanted stents (Table 1). However, patients in the NSTE-ACS group did have

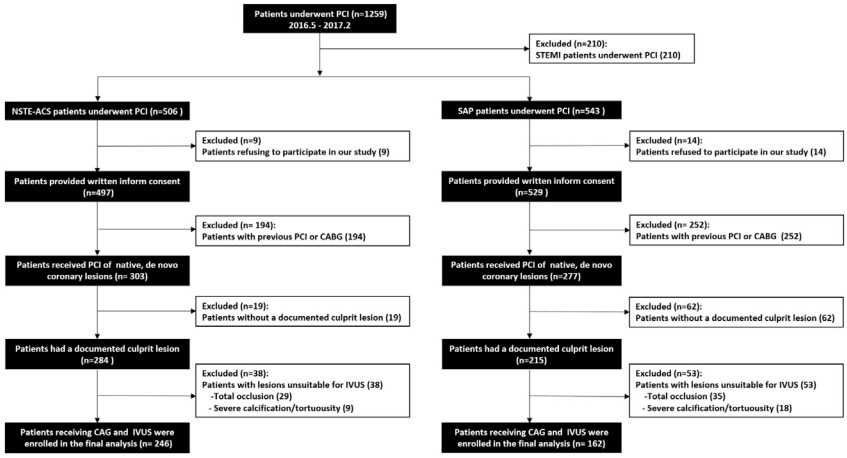

Fig. 1. Flow chart of patient enrollment. CABG, coronary artery bypass graft; CAG, coronary artery angiography; NSTE-ACS, non-ST-segment elevation acute coronary syndrome; IVUS, intravascular ultrasound; PCI, percutaneous coronary intervention; SAP, stable angina pectoris.

poorer epicardial flow (pre-TIMI 0–2, 45.1% vs 5.6%, $P < 0.0001$) as well as impaired tissue-level perfusion (pre-TMPG 0–2, 54.9% vs 9.3%, $P < 0.0001$) before PCI.

3.2. Plaque characteristics comparison of NSTE-ACS group vs SAP group

The IVUS results of grayscale and iMap for NSTE-ACS and SAP groups were shown in Table 2. Positive remodeling at the MLA sites was more common in patients with NSTE-ACS vs SAP (67.7% vs 31.5%, $P < 0.0001$). Furthermore, patients with NSTE-ACS more often had echo-attenuated plaques and plaque rupture than SAP patients (echo-attenuated plaques, 39.0% vs 11.1%, $P = 0.0004$; plaque rupture, 51.2% vs 18.5%, $P = 0.0001$).

Analysis of the plaque composition at the MLA sites demonstrated that NC% in patients with NSTE-ACS was significantly higher than in SAP (22.3 ± 9.2% vs 17.3 ± 8.7%, $P = 0.002$). Furthermore, a smaller percentage of the fibrous component was found at the MLA sites in patients with NSTE-ACS than in patients with SAP (51.9 ± 12.1% vs 59.5 ± 12.2%, $P = 0.003$). There was no significant difference between the 2 groups for the other plaque components.

In addition, analysis of the plaque composition within the entire length of \ culprit lesions showed a significant difference in the percentage of necrotic and fibrous component between the 2 groups. The culprit plaques of patients with NSTE-ACS contained a larger NC% and a smaller percentage of the fibrous component than those with SAP (NC%: 20.8 ± 7.9% vs 15.9 ± 7.2%, $P = 0.0004$; fibrous component: 55.0 ± 12.4% vs 60.8 ± 10.3%, $P = 0.005$). No significant difference between the 2 groups was detected for the other plaque components of the entire culprit lesion.

Table 1
Baseline characteristics of patients (NSTE-ACS vs. SAP).

Characteristic	NSTE-ACS (patients = 246)	SAP (patients = 162)	*P*-value
Age, years	63.8 ± 11.3	66.2 ± 12.2	0.243
Female gender, n (%)	30(12.2)	30(18.5)	0.078
Hypertension, n (%)	126(51.2)	96(59.3)	0.111
Diabetes mellitus, n (%)	60(24.4)	48 (29.6)	0.241
Hypercholesterolemia, n (%)	54(22.0)	48 (29.6)	0.080
Current smoking, n (%)	141(57.3)	60(37.0)	<0.001
Family history, n (%)	30(12.2)	13(8.0)	0.179
Peripheral vascular disease, n (%)	15(6.1)	6(3.7)	0.284
Previous myocardial infarction, n (%)	15(6.1)	6(3.7)	0.284
Previous stroke, n (%)	12(4.9)	6(3.7)	0.572
Left ventricle ejection fraction (%)	51.8 ± 12.7	58.4 ± 10.5	0.002
Target coronary artery, n (%)			0.740
Left main	3(1.2)	3(1.9)	
Left anterior descending	120(48.8)	90(55.6)	
Left circumflex	33(13.4)	18(11.1)	
Right	90(36.6)	51(31.5)	
Stent implantation, n (%)	240(97.6)	156(96.3)	0.553
Implanted stents, n	1.2 ± 0.5	1.2 ± 0.6	0.721
Stent size (mm)	3.3 ± 0.5	3.2 ± 0.5	0.314
Stent length (mm)	17.8 ± 5.8	16.3 ± 6.7	0.189
Pre-TIMI (0–2)	111(45.1)	9(5.6)	<0.001
Pre-TMPG (0–2)	135(54.9)	15(9.3)	<0.001

Data presented as mean ± SD or number (n) and percentage (%) of patients. NSTE-ACS indicates non-ST-segment elevation acute coronary syndrome; SAP, stable angina pectoris; TIMI, Thrombolysis In Myocardial Infarction. TMPG, TIMI myocardial perfusion grade.

3.3. Association of plaque characteristics with epicardial perfusion in NSTE-ACS patients

To evaluate the relationship between plaque components and epicardial coronary flow after PCI in NSTE-ACS patients, we divided all NSTE-ACS patients into two groups based upon post-PCI TIMI grade: one group for patients with TFG 0–2 and the other for patients with TFG 3. The gray-scale and iMap-IVUS data were shown in Table 2. Patients with TFG 0–2 had larger EEM CSA and P&M CSA at the MLA sites. Qualitative data showed no significant difference between 2 groups. Plaque composition at the MLA sites showed a higher NC% in patients with TFG 0–2 (29.7 ± 8.0% vs 21.0 ± 8.8%, $P = 0.002$). A smaller percentage of the fibrous component was observed at the MLA sites in patients with TFG 0–2 than in patients with TFG 3 (44.7 ± 11.9% vs 54.3 ± 12.3%, $P = 0.014$). There was no significant difference between the 2 groups for the other plaque components. Analysis of the plaque composition of the entire culprit lesions showed a result similar with that of the MLA sites.

3.4. Association of plaque characteristics with myocardial tissue-level perfusion in NSTE-ACS patients

We further assessed the relationship between plaque components and post-PCI myocardial tissue-level perfusion (TMPG and TMPFC) in NSTE-ACS patients. Table 3 listed gray-scale and iMap-IVUS results of different TMPG groups. In the grayscale IVUS analysis patients with TMPG 0–2 had larger EEM CSA and P&M CSA at the MLA site along with a heavier plaque burden, but a smaller MLA than patients with TMPG 3. The NC% in the TMPG 0–2 group was significantly higher both at the MLA site and within the entire lesion (MLA, 26.2 ± 8.8% vs 19.6 ± 8.3, $P = 0.003$; the entire lesion, 25.0 ± 8.1% vs 18.4 ± 6.7%, $P = 0.0001$).

To confirm the relationship between plaque components and post-PCI myocardial tissue-level perfusion, we further used TMPFC, a novel quantitative angiographic method, to assess myocardial tissue-level

Table 2
Grayscale and iMap-IVUS findings (NSTE-ACS vs. SAP & TFG0–2 vs. TFG3).

Characteristic	NSTE-ACS ($n = 246$)	SAP ($n = 162$)	*P*-value	TFG 0–2 ($n = 36$)	TFG 3 ($n = 210$)	*P*-value
Grayscale IVUS data						
Quantitative grayscale data						
Lumen CSA (mm^2)	3.4 ± 0.6	3.3 ± 0.7	0.354	3.2 ± 0.7	3.5 ± 0.6	0.294
EEM CSA (mm^2)	16.2 ± 4.4	15.1 ± 4.8	0.149	18.9 ± 4.1	15.7 ± 4.2	0.021
P&M CSA (mm^2)	12.8 ± 4.4	11.7 ± 4.7	0.192	15.6 ± 4.6	12.3 ± 4.2	0.015
Plaque burden (%)	77.1 ± 7.7	75.6 ± 9.8	0.316	80.9 ± 9.9	76.5 ± 7.2	0.066
Remodeling index	1.8 ± 0.1	1.0 ± 0.1	0.022	1.1 ± 0.1	1.1 ± 0.1	0.103
Positive remodeling (%)	155(67.7)	51(31.5)	<0.0001	30(83.3)	135(64.3)	0.320
Lesion length (mm)	14.6 ± 7.7	16.4 ± 9.3	0.438	15.3 ± 8.5	13.8 ± 7.1	0.287
Plaque volume (mm^3)	110.9 ± 65.2	98.7 ± 55.4	0.107	120.3 ± 69.3	100.2 ± 60.4	0.042
Qualitative grayscale data						
Plaque rupture (%)	126(51.2)	30(18.5)	<0.001	28(75.0)	99(47.1)	0.001
Echo-lucent plaques (%)	45(18.3)	20(12.3)	0.108	9(25.0)	36(17.1)	0.260
Echo-attenuated plaques (%)	96(39.0)	18(11.1)	<0.001	24(66.7)	72(34.3)	<0.001
Calcified plaques (%)	78(31.7)	52(37.0)	0.266	12(33.3)	66(31.4)	0.820
iMap–IVUS parameters						
Plaque composition at MLA						
Fibrous (%)	51.9 ± 12.1	59.5 ± 12.2	0.003	44.7 ± 11.9	54.3 ± 12.3	0.014
Lipid (%)	11.4 ± 5.7	9.9 ± 5.0	0.111	12.7 ± 6.2	11.2 ± 5.6	0.397
Necrotic (%)	22.3 ± 9.2	17.3 ± 8.7	0.002	29.7 ± 8.0	21.0 ± 8.8	0.002
Calcified (%)	6.3 ± 5.0	7.4 ± 5.0	0.205	5.7 ± 5.1	6.4 ± 5.0	0.658
Plaque composition over lesion						
Fibrous (%)	55.0 ± 12.4	60.8 ± 10.3	0.005	46.5 ± 9.2	56.4 ± 12.4	0.010
Lipid (%)	10.2 ± 4.8	9.6 ± 4.0	0.399	11.7 ± 4.5	10.0 ± 4.8	0.239
Necrotic (%)	20.8 ± 7.9	15.9 ± 7.2	0.0004	27.9 ± 7.3	19.6 ± 7.4	0.001
Calcified (%)	6.5 ± 3.7	7.8 ± 4.5	0.077	6.3 ± 4.1	6.5 ± 3.7	0.868

Data presented as mean ± SD or number (n) and percentage (%) of patients. CSA indicates cross-sectional area; EEM, external elastic membrane; IVUS, intravascular ultrasound; MLA, minimum lumen Area; NSTE-ACS indicates non-ST-segment elevation acute coronary syndrome; P&M = plaque&media; SAP, stable angina pectoris; TMPFC, TIMI myocardial perfusion frame count; TMPG, TIMI myocardial perfusion grade.

perfusion [1,2] as shown in Table 3. In the grayscale IVUS analysis, NSTE-ACS patients with abnormal TMPFC had heavier plaque burden, more echo-attenuated plaques, and larger lumen EEM CSA and P&M CSA. Similar to the results in the TMPG comparison, patients with abnormal TMPFC had larger NC% and less fibrous percentage both at the MLA site and within the entire lesion (NC% at MLA site, 24.6 ± 9.4% vs 20.1 ± 8.5%, $P = 0.025$; fibrous percentage at MLA site, 49.3 ± 11.9% vs 56.1 ± 12.6%, $P = 0.014$; necrotic percentage within the entire lesion, 25.6 ± 7.2% vs 16.4 ± 5.6%, $P < 0.0001$; fibrous percentage within the entire lesion, 48.8 ± 11.3% vs 60.6 ± 10.7%, $P < 0.0001$). We further

Table 3
Grayscale and iMap-IVUS findings (TMPG0–2 vs. TMPG3 & TMPFC > 90 vs. TMPFC ≤ 90).

Characteristic	TMPG 0–2 ($n = 90$)	TMPG 3 ($n = 156$)	*P*-value	TMPFC >90 ($n = 117$)	TMPFC ≤90 ($n = 129$)	*P*-value
Grayscale IVUS data						
Quantitative grayscale data						
Lumen CSA (mm^2)	3.2 ± 0.7	3.5 ± 0.6	0.037	3.3 ± 0.7	3.5 ± 0.6	0.282
EEM CSA (mm^2)	17.6 ± 4.6	15.4 ± 4.0	0.032	17.6 ± 4.5	14.9 ± 3.8	0.004
P&M CSA (mm^2)	14.3 ± 4.8	11.9 ± 3.9	0.015	14.3 ± 4.6	11.4 ± 3.8	0.003
Plaque burden (%)	79.7 ± 8.6	75.7 ± 6.8	0.022	79.3 ± 8.4	75.2 ± 6.6	0.017
Remodeling index	1.1 ± 0.1	1.1 ± 0.2	0.195	1.1 ± 0.1	1.1 ± 0.1	0.428
Positive remodeling (%)	57(63.3)	108(69.2)	0.584	84(71.8)	81(62.8)	0.386
Lesion length (mm)	15.4 ± 5.7	14.0 ± 8.7	0.305	14.9 ± 9.1	14.1 ± 7.9	0.437
Plaque volume (mm^3)	121.9 ± 65.2	98.9 ± 70.2	0.031	118.9 ± 57.2	101.5 ± 63.9	0.046
Qualitative grayscale data						
Plaque rupture (%)	57(63.3)	69(44.2)	0.004	72(61.5)	54(41.9)	0.002
Echo-lucent plaques (%)	21(23.3)	24(15.4)	0.120	26(22.2)	19(14.7)	0.129
Echo-attenuated plaques (%)	54(60.0)	42(26.9)	<0.001	60(51.3)	36(27.9)	<0.001
Calcified plaques (%)	27(30.0)	51(32.7)	0.662	33(28.2)	45(34.9)	0.261
iMap–IVUS parameters						
Plaque composition at MLD						
Fibrous (%)	47.5 ± 11.6	56.0 ± 12.3	0.003	49.3 ± 11.9	56.1 ± 12.6	0.014
Lipid (%)	12.7 ± 6.8	10.6 ± 4.9	0.141	12.8 ± 6.5	10.2 ± 4.6	0.085
Necrotic (%)	26.2 ± 8.8	19.6 ± 8.3	0.003	24.6 ± 9.4	20.1 ± 8.5	0.025
Calcified (%)	5.7 ± 4.5	6.6 ± 5.3	0.416	6.2 ± 5.5	6.3 ± 4.6	0.883
Plaque composition over lesion						
Fibrous (%)	48.8 ± 11.9	58.6 ± 11.4	0.0004	48.8 ± 11.3	60.6 ± 10.7	<0.0001
Lipid (%)	11.7 ± 4.9	9.4 ± 4.5	0.077	11.2 ± 4.8	9.3 ± 4.6	0.063
Necrotic (%)	25.0 ± 8.1	18.4 ± 6.7	0.0001	25.6 ± 7.2	16.4 ± 5.6	<0.0001
Calcified (%)	7.0 ± 3.7	6.2 ± 3.8	0.378	6.8 ± 4.0	6.2 ± 3.6	0.481

Data presented as mean ± SD or number (n) and percentage (%) of patients. CSA indicates cross-sectional area; EEM, external elastic membrane; IVUS, intravascular ultrasound; MLA, minimum lumen Area; NSTE-ACS indicates non-ST-segment elevation acute coronary syndrome; P&M = plaque&media; SAP, stable angina pectoris; TFG, TIMI flow grade.

performed linear regression of TMPFC vs NC% within the entire plaque: $r = 0.712$, $P < 0.0001$ (Fig. 2-B).

3.5. Determinants of abnormal myocardial tissue-level perfusion

To determine independent predictors related to the impaired microvascular perfusion, we performed multivariable analyses of baseline variables with a univariate $P \leq 0.10$ and variables known to be related to myocardial perfusion. Fig. 2-C1 showed that age ≥75 years (OR 3.48 [95%CI 1.93–6.26], $P < 0.001$), echo-attenuated plaques (OR 3.02 [95% CI 1.86–4.91], $P = 0.003$) and NC% volume (OR 2.39 [95% CI 1.60–3.57], $P = 0.009$) were independently associated with reduced post-PPCI TMPG. Age ≥75 years (OR 3.11[95%CI 1.91–5.05], $P < 0.001$), NC% volume (OR 2.89 [95% CI 1.62–5.16], $P = 0.008$), echo-attenuated plaques (OR 2.32 [95% CI 1.56–3.45], $P = 0.011$), and diabetes mellitus (OR 1.95 [95%CI 1.05–3.62], $P = 0.042$) were independent predictors of abnormal post-PPCI TMPFC (Fig. 2-C2).

3.6. Optimal threshold to predict abnormal myocardial tissue-level perfusion

The ROC curve showed that 20.09% was the optimal threshold of NC % of the entire lesion to predict impaired TMPG (area under the curve [AUC] = 0.75, 95% CI 0.63–0.86, $P = 0.001$; sensitivity, 65.4%, specificity, 76.9%; Fig. 2-D1), and 21.03% was the optimal cut point of NC% volume to predict impaired TMPFC (AUC = 0.88, 95%CI: 0.79–0.96, $P = 0.001$; sensitivity, 82.1%, specificity, 88.4%; Fig. 2-D2).

4. Discussion

The IMAP-ACS study assessed the impact of culprit lesion plaque composition on coronary reperfusion (i.e., TFG) and microvascular reperfusion (i.e., TMPG and TMPFG) in NSTE-ACS patients. The main findings of our study were as follows: 1) Using the iMap imaging system, NSTE-ACS patients were found to have more necrotic plaques in

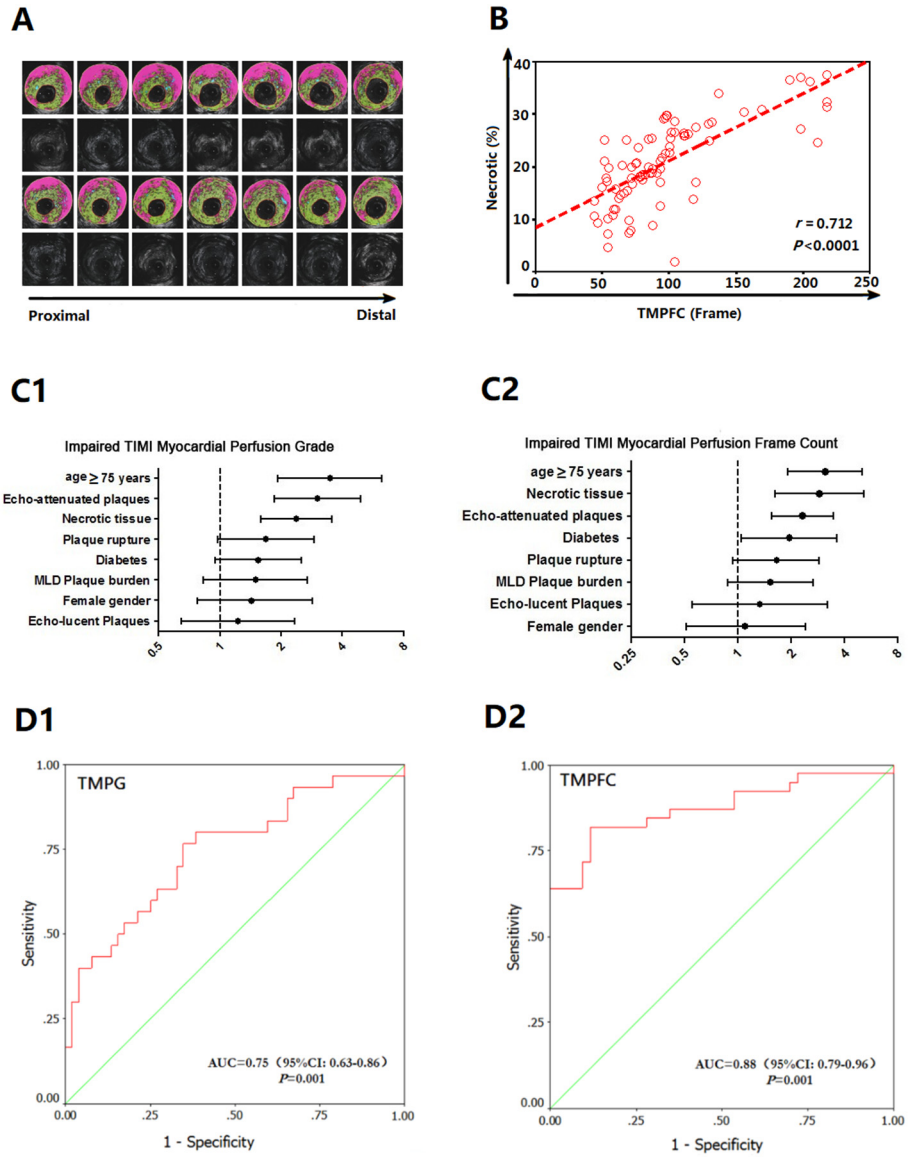

Fig. 2. The relationship between culprit plaque characteristics and myocardial tissue-level perfusion in NSTE-ACS patients. A, Representative iMap-intravascular ultrasound images with abnormal myocardial tissue-level perfusion. B, Correlation between iMap–IVUS-derived percentage of necrotic tissue and TIMI Myocardial Perfusion Frame Count (TMPFC) in NSTE-ACS patients undergoing PCI. C, Independent predictors of impaired TIMI Myocardial Perfusion Grade (TMPG, C1) and TIMI Myocardial Perfusion Frame Count (TMPFC, C2). D, ROC curve to determine the optimal cutoff value for the percentage of necrotic tissue to impaired TIMI Myocardial Perfusion Grade (TMPG, D1) and TIMI Myocardial Perfusion Frame Count (TMPFC, D2). CABG, coronary artery bypass graft; CAG, coronary artery angiography; NSTE-ACS, non-ST-segment elevation acute coronary syndrome; IVUS, PCI, percutaneous coronary intervention.

culprit lesions than SAP patients; 2) NSTE-ACS patients with post-PCI impaired epicardial perfusion (TFG 0–2) had more necrotic plaques; 3) A greater percentage of the NC component was also observed in NSTE-ACS patients with insufficient myocardial tissue-level perfusion (TMPG 0–2 or TMPFC>90); 4) Multivariate analyses identified iMap-derived NC as an independent predictor of myocardial tissue-level perfusion with an optimal cut-points of iMap-derived %NC volume of ≈20% to predict impaired TMPG and TMPFC.

Plaque composition is considered to be a key determinant of the propensity of atherosclerotic lesions to provoke clinical events [18–23]. Previous studies suggested that assessment of the angiographic severity of a coronary stenosis may be inadequate to accurately predict a subsequent acute coronary event. The development of multiple intracoronary imaging modalities has increased our understanding of coronary atherosclerotic disease. In fact, a wide range of information arising from a variety of intravascular imaging modalities such as IVUS, optical coherence tomography (OCT), and more recently, near-infrared spectroscopy (NIRS) developed the concept of the plaque tissue characteristics and its relationship to acute coronary syndromes [24].

The iMap-IVUS was the most recent radiofrequency IVUS imaging technique for assessing plaque tissue characteristics. Ex vivo validation demonstrated accuracies of 97%, 98%, 95%, and 98% for necrotic, lipidic, fibrotic and calcified regions, respectively [11]. Compared with gray-scale IVUS, iMap-IVUS makes it possible to determine not only tissue characterization, but also the absolute plaque volume and the ratio as well as the plaque area in lesions of interest [25]. In this intracoronary imaging study coronary plaque composition was compared between patients with NSTE-ACS and those with SAP. The amounts of the iMap-derived NC component were larger and the amounts of fibrotic plaque were less in patients with NSTE-ACS, consistent with previous virtual histology IVUS (VH-IVUS) studies [26]. Moreover, a positive correlation was observed between the extent of lipid-rich plaque measured by NIRS and IVUS-derived plaque burden [27].

Several VH-IVUS studies have focused on the association between plaque composition and epicardial coronary reperfusion (epicardial-level perfusion) in ACS patients. The VH-IVUS study by Hong et al. demonstrated that ACS patients with abnormal epicardial reflow (TIMI flow 0–2) had more NC rich lesions compared with ACS patients with TIMI flow 3 after stent deployment [6]. On the contrary, Bae et al. showed that abnormal epicardial reflow was relevant to high VH-IVUS fibro-fatty and fibrotic volume of the culprit lesion rather than the NC in patients undergoing primary PCI [25]. In our study, the necrotic component identified by iMap-IVUS was significantly larger while the fibrous component was smaller in NSTE-ACS patients with abnormal epicardial-level perfusion than in those with normal epicardial reflow both at the MLA site and within the entire lesion. Moreover, we observed that NSTE-ACS patients with impaired myocardial tissue-level reperfusion had more necrotic plaques. Up to now, few studies have discussed the association between plaque composition and myocardial tissue-level perfusion. Using OCT, Tanaka et al. showed that post TIMI blush grade also was more likely to be poor in NSTE-ACS patients with lipid-rich plaque [28]. In our study, microvascular flow was measured by two methods. One was the TMPG, an angiographic surrogate of myocardial perfusion developed by Gibson et al. that focuses on the velocity of contrast opacity clearance, which was categorical and operator dependent [13]; and the other was the TMPFC, which quantified myocardial perfusion by timing the filling and clearance of contrast in the myocardium using cine-angiographic frame-counting [1,2].

We observed that NSTE-ACS patients with impaired myocardial microvascular reperfusion (i.e., impaired TMPG and TMPFC) had a larger necrotic component. To determine whether this was truly related to impaired microvascular perfusion, we first used a linear regression model which confirmed a positive correlation between the amount of the necrotic component and TMPFC. Besides, we performed multivariate logistic analysis, which showed that necrotic component was an independent predictor both of TMPG and TMPFC after PCI. The development of poor myocardial perfusion was considered to result from microvascular damage produced by microvascular obstruction or reperfusion injury [29]. It is believed that fragile tissues contained in the necrotic components could be easily liberated as small emboli by mechanical fragmentation during coronary stenting which eventually induces abnormal reperfusion. The cellular debris, cholesterol crystals, and intramural bleeding of the necrotic component all could induce distal embolization. Thus, prediction of impaired myocardial reperfusion with iMap-IVUS might have a substantial impact on decision making in the catheterization laboratory.

4.1. Study limitations

Several limitations of our study should be considered to place its findings in the proper context. First, although data in our study was prospectively collected and blindly analyzed, the sample size was relatively small. Second, we only included NSTE-ACS patients, so the association between plaque composition and myocardial tissue-level perfusion in STEMI patients remained unclear. Third, although iMap-IVUS had a predictive accuracy of >95% for tissue characterization in ex vivo studies [11], further studies with other intravascular imaging modalities such as OCT and NIRS are warranted to validate the results of the current study. Fourth, although microvascular flow in our study was measured by both TMPG (an semi-quantitative angiographic index of myocardial perfusion [13]) and TMPFC (a quantitative index developed by our group with the aim to quantify TMPG and assess myocardial perfusion objectively [1,2]), new modality such as cardiac magnetic resonance imaging has great potential for the assessment of myocardial reperfusion injury and might be used in future studies [1,2]. Fifth, the measurements of the iMap-derived necrotic fraction over the entire lesion needed offline analysis. To translate this to daily practice, software should be developed to calculate the percentages of each component over the entire culprit lesion in a real-time manner during PCI procedure. Finally, the comparison of the plaque characteristics between 246 NSTE-ACS and 162 SAP patients in the present study might introduce potential selection bias.

5. Conclusions

Larger necrotic component within coronary plaques may have higher risks of developing acute coronary events and having impaired coronary reperfusion and microvascular reperfusion post-PCI. For ACS patients with high necrotic component coronary plaques, more therapies were needed to prevent postprocedural abnormal myocardial reperfusion, including intracoronary drugs administration such as glycoprotein IIb/IIIa receptor antagonists, nitroprusside, verapamil or nicorandil [30,31].

Conflicts of interest

Nothing to report.

Acknowledgement

This work was supported by National Key Research and Development Program of China (2016YFC1301203 and 2018YFC1312802), National Science Fund for Distinguished Young Scholars (81625002), Shanghai Outstanding Academic Leaders Program (18XD1402400), Shanghai Shen Kang Hospital Development Center (16CR3034A) and Shanghai Jiao Tong University (YG2016MS45 and YG2015ZD04).

Appendix A. Supplementary data

Supplementary data to this article can be found online at https://doi.org/10.1016/j.ijcard.2019.02.010.

References

[1] S. Ding, J. Pu, Z.Q. Qiao, P. Shan, W. Song, Y. Du, J.Y. Shen, S.X. Jin, Y. Sun, L. Shen, Y.L. Lim, B. He, TIMI myocardial perfusion frame count: a new method to assess myocardial perfusion and its predictive value for short-term prognosis, Catheter. Cardiovasc. Interv. 75 (2010) 722–732.

[2] J. Pu, S. Ding, H. Ge, Y. Han, J. Guo, R. Lin, X. Su, H. Zhang, L. Chen, B. He, EARLY-MYO Investigators, Efficacy and safety of a pharmaco-invasive strategy with half-dose alteplase versus primary angioplasty in ST-segment-elevation myocardial infarction: EARLY-MYO trial (early routine catheterization after alteplase fibrinolysis versus primary PCI in acute ST-segment-elevation myocardial infarction), Circulation 136 (2017) 1462–1473.

[3] X. Sheng, S. Ding, H. Ge, Y. Sun, L. Kong, J. He, J. Pu, B. He, Intracoronary infusion of alprostadil and nitroglycerin with targeted perfusion microcatheter in STEMI patients with coronary slow flow phenomenon, Int. J. Cardiol. 265 (2018) 6–11.

[4] C.M. Gibson, C.P. Cannon, S.A. Murphy, S.J. Marble, H.V. Barron, E. Braunwald, Relationship of the TIMI myocardial perfusion grades, flow grades, frame count, and percutaneous coronary intervention to long-term outcomes after thrombolytic administration in acute myocardial infarction, Circulation 105 (2002) 1909–1913.

[5] C.O. Costantini, G.W. Stone, R. Mehran, E. Aymong, C.L. Grines, D.A. Cox, T. Stuckey, M. Turco, B.J. Gersh, J.E. Tcheng, E. Garcia, J.J. Griffin, G. Guagliumi, M.B. Leon, A.J. Lansky, Frequency, correlates, and clinical implications of myocardial perfusion after primary angioplasty and stenting, with and without glycoprotein IIb/IIIa inhibition, in acute myocardial infarction, J. Am. Coll. Cardiol. 44 (2004) 305–312.

[6] Y.J. Hong, M.H. Jeong, Y.H. Choi, J.S. Ko, M.G. Lee, W.Y. Kang, S.E. Lee, S.H. Kim, K.H. Park, D.S. Sim, N.S. Yoon, H.J. Youn, K.H. Kim, H.W. Park, J.H. Kim, Y. Ahn, J.G. Cho, J.C. Park, J.C. Kang, Impact of plaque components on no-reflow phenomenon after stent deployment in patients with acute coronary syndrome: a virtual histology-intravascular ultrasound analysis, Eur. Heart J. 32 (2011) 2059–2066.

[7] J. Pu, G.S. Mintz, E.S. Brilakis, S. Banerjee, A.R. Abdel-Karim, B. Maini, S. Biro, J.B. Lee, G.W. Stone, G. Weisz, A. Maehara, In vivo characterization of coronary plaques: novel findings from comparing greyscale and virtual histology intravascular ultrasound and near-infrared spectroscopy, Eur. Heart J. 33 (2012) 372–383.

[8] B.E. Claessen, A. Maehara, M. Fahy, K. Xu, G.W. Stone, G.S. Mintz, Plaque composition by intravascular ultrasound and distal embolization after percutaneous coronary intervention, JACC Cardiovasc. Imaging 5 (2012) 111–118.

[9] R. Iijima, H. Shinji, N. Ikeda, H. Itaya, K. Makino, A. Funatsu, I. Yokouchi, H. Komatsu, N. Ito, H. Nuruki, R. Nakajima, M. Nakamura, Comparison of coronary arterial finding by intravascular ultrasound in patients with "transient no-reflow" versus "reflow" during percutaneous coronary intervention in acute coronary syndrome, Am. J. Cardiol. 97 (2006) 29–33.

[10] T. Katayama, N. Kubo, Y. Takagi, H. Funayama, N. Ikeda, T. Ishida, T. Hirahara, Y. Sugawara, T. Yasu, M. Kawakami, M. Saito, Relation of atherothrombosis burden and volume detected by intravascular ultrasound to angiographic no-reflow phenomenon during stent implantation in patients with acute myocardial infarction, Am. J. Cardiol. 97 (2006) 301–304.

[11] S. Sathyanarayana, S. Carlier, W. Li, L. Thomas, Characterisation of atherosclerotic plaque by spectral similarity of radiofrequency intravascular ultrasound signals, EuroIntervention 5 (2009) 133–139.

[12] Effects of tissue plasminogen activator and a comparison of early invasive and conservative strategies in unstable angina and non-Q-wave myocardial infarction. Results of the TIMI IIIB trial. Thrombolysis in myocardial ischemia, Circulation 89 (1994) 1545–1556.

[13] C.M. Gibson, C.P. Cannon, S.A. Murphy, K.A. Ryan, R. Mesley, S.J. Marble, C.H. McCabe, F. Van De Werf, E. Braunwald, Relationship of TIMI myocardial perfusion grade to mortality after administration of thrombolytic drugs, Circulation 101 (2000) 125–130.

[14] G.S. Mintz, S.E. Nissen, W.D. Anderson, S.R. Bailey, R. Erbel, P.J. Fitzgerald, F.J. Pinto, K. Rosenfield, R.J. Siegel, E.M. Tuzcu, P.G. Yock, American College of Cardiology Clinical Expert Consensus document on standards for acquisition, measurement and reporting of Intravascular Ultrasound Studies (IVUS). A report of the American College of Cardiology Task Force on clinical expert consensus documents, J. Am. Coll. Cardiol. 37 (2001) 1478–1492.

[15] J. Pu, G.S. Mintz, S. Biro, J.B. Lee, S.T. Sum, S.P. Madden, A.P. Burke, P. Zhang, B. He, J.A. Goldstein, G.W. Stone, J.E. Muller, R. Virmani, A. Maehara, Insights into echo-attenuated plaques, echolucent plaques, and plaques with spotty calcification: novel findings from comparisons among intravascular ultrasound, near-infrared spectroscopy, and pathological histology in 2294 human coronary artery segments, J. Am. Coll. Cardiol. 63 (2014) 2220–2233.

[16] X.Y. Zhao, X.F. Wang, L. Li, J.Y. Zhang, Y.Y. Du, H.M. Yao, Plaque characteristics and serum pregnancy-associated plasma protein A levels predict the no-reflow phenomenon after percutaneous coronary intervention, J. Int. Med. Res. 41 (2013) 307–316.

[17] S. Ding, L. Xu, F. Yang, L. Kong, Y. Zhao, L. Gao, W. Wang, R. Xu, H. Ge, M. Jiang, J. Pu, B. He, Association between tissue characteristics of coronary plaque and distal embolization after coronary intervention in acute coronary syndrome patients: insights from a meta-analysis of virtual histology-intravascular ultrasound studies, PLoS One 9 (2014), e106583.

[18] R. Virmani, F.D. Kolodgie, A.P. Burke, A. Farb, S.M. Schwartz, Lessons from sudden coronary death: a comprehensive morphological classification scheme for atherosclerotic lesions, Arterioscler. Thromb. Vasc. Biol. 20 (2000) 1262–1275.

[19] R. Virmani, A.P. Burke, F.D. Kolodgie, A. Farb, Vulnerable plaque: the pathology of unstable coronary lesions, J. Interv. Cardiol. 15 (2002) 439–446.

[20] R. Virmani, A.P. Burke, A. Farb, F.D. Kolodgie, Pathology of the vulnerable plaque, J. Am. Coll. Cardiol. 47 (2006) 13–18.

[21] M. Naghavi, P. Libby, E. Falk, S.W. Casscells, S. Litovsky, J. Rumberger, J.J. Badimon, C. Stefanadis, P. Moreno, G. Pasterkamp, Z. Fayad, P.H. Stone, S. Waxman, P. Raggi, M. Madjid, A. Zarrabi, A. Burke, C. Yuan, P.J. Fitzgerald, S. Kaul, H. Drexler, P. Greenland, J.E. Muller, R. Virmani, P.M. Ridker, D.P. Zipes, P.K. Shah, J.T. Willerson, From vulnerable plaque to vulnerable patient: a call for new definitions and risk assessment strategies: part II, Circulation 108 (2003) 1772–1778.

[22] J.T. Motz, M. Fitzmaurice, A. Miller, S.J. Gandhi, A.S. Haka, L.H. Galindo, R.R. Dasari, J.R. Kramer, M.S. Feld, In vivo Raman spectral pathology of human atherosclerosis and vulnerable plaque, J. Biomed. Opt. 11 (2006), 021003.

[23] N.L. Lysova, O.A. Trusov, A.I. Shchegolev, O.D. Mishnev, The anatomical pathology of a vulnerable atherosclerotic plaque in ischemic heart disease, Arkh. Patol. 69 (2007) 22–25.

[24] R. Nakazato, H. Otake, A. Konishi, M. Iwasaki, B.-K. Koo, H. Fukuya, T. Shinke, K.-I. Hirata, J. Leipsic, D.S. Berman, J.K. Min, Atherosclerotic plaque characterization by CT angiography for identification of high-risk coronary artery lesions: a comparison to optical coherence tomography, Eur. Heart J. Cardiovasc. Imaging 16 (2015) 373–379.

[25] J.H. Bae, T.G. Kwon, D.W. Hyun, C.S. Rihal, A. Lerman, Predictors of slow flow during primary percutaneous coronary intervention: an intravascular ultrasound-virtual histology study, Heart 94 (2008) 1559–1564.

[26] M.K. Hong, G.S. Mintz, C.W. Lee, J. Suh, J.H. Kim, D.W. Park, S.W. Lee, Y.H. Kim, S.S. Cheong, J.J. Kim, S.W. Park, S.J. Park, Comparison of virtual histology to intravascular ultrasound of culprit coronary lesions in acute coronary syndrome and target coronary lesions in stable angina pectoris, Am. J. Cardiol. 100 (2007) 953–959.

[27] T. Dohi, A. Maehara, P.R. Moreno, U. Baber, J.C. Kovacic, A.M. Limaye, Z.A. Ali, J.M. Sweeny, R. Mehran, G.D. Dangas, K. Xu, S.K. Sharma, G.S. Mintz, A.S. Kini, The relationshipamong extent of lipid-rich plaque, lesion characteristics, and plaque progression/regression in patients with coronary artery disease: a serial near-infrared spectroscopy and intravascular ultrasound study, Eur. Heart J. Cardiovasc. Imaging 16 (2015) 81–87.

[28] A. Tanaka, T. Imanishi, H. Kitabata, T. Kubo, S. Takarada, T. Tanimoto, A. Kuroi, H. Tsujioka, H. Ikejima, K. Komukai, H. Kataiwa, K. Okouchi, M. Kashiwaghi, K. Ishibashi, H. Matsumoto, K. Takemoto, N. Nakamura, K. Hirata, M. Mizukoshi, T. Akasaka, Lipid-rich plaque and myocardial perfusion after successful stenting in patients with non-ST-segment elevation acute coronary syndrome: an optical coherence tomography study, Eur. Heart J. 30 (2009) 1348–1355.

[29] F. Alfayoumi, V. Srinivasan, M. Geller, A. Gradman, The no-reflow phenomenon: epidemiology, pathophysiology, and therapeutic approach, Rev. Cardiovasc. Med. 6 (2005) 72–83.

[30] H. Matsuo, S. Watanabe, T. Watanabe, Prevention of no-reflow/slow-flow phenomenon during rotational atherectomy–a prospective randomized study comparing intracoronary continuous infusion of verapamil and nicorandil, Am. Heart J. 154 (2007) 994.

[31] N. Shinozaki, H. Ichinose, K. Yahikozawa, H. Shimada, K. Hoshino, Selective intracoronary administration of nitroprusside before balloon dilatation prevents slow reflow during percutaneous coronary intervention in patients with acute myocardial infarction, Int. Heart J. 48 (2007) 423–433.